Open access • Journal Article • DOI:10.1063/1.1647267

Cathodoluminescence of defects in sintered tin oxide — Source link

David Maestre, Ana Cremades, Javier Piqueras

Published on: 02 Mar 2004 - Journal of Applied Physics (American Institute of Physics)

Topics: Cathodoluminescence, Scanning electron microscope, Tin oxide and Luminescence

Cathodoluminescence of defects in sintered tin oxide

D. Maestre, A. Cremades, and J. Piqueras

Citation: J. Appl. Phys. **95**, 3027 (2004); doi: 10.1063/1.1647267
View online: http://dx.doi.org/10.1063/1.1647267
View Table of Contents: http://jap.aip.org/resource/1/JAPIAU/v95/i6
Published by the American Institute of Physics.

Cathodoluminescence of defects in sintered tin oxide

D. Maestre, A. Cremades,[a] and J. Piqueras
Departamento de Física de Materiales, Facultad de Ciencias Físicas, Universidad Complutense, 28040 Madrid, Spain

(Received 24 October 2003; accepted 18 December 2003)

Cathodoluminescence (CL) in the scanning electron microscope (SEM) has been used to investigate the luminescence mechanisms in tin oxide. Sintered material prepared from high purity powder has been found to show a strong dependence of the CL emission on the thermal treatments applied during sample preparation. SEM images show the presence of nano and microcrystalline grains. The correlation of the grain size and morphology with the optical emission is analyzed by CL microscopy and spectroscopy. The main emission bands appear centered at about 2.58, 2.25, and 1.94 eV depending on the sintering treatment. CL images reveal that the 2.25 and the 2.58 eV bands are associated at specific crystal faces. The evolution of the luminescence bands with mechanical milling shows a complex evolution of the 1.94 and 2.58 eV emissions which is explained by formation and recovery of defects during milling. © *2004 American Institute of Physics.*
[DOI: 10.1063/1.1647267]

I. INTRODUCTION

One of the reasons for the increasing interest in semiconducting oxides like SnO_2, TiO_2, $LaFeO_3$, $SmFeO_3$ and In_2O_3 is the application of nanocrystalline powders for gas sensing and gas monitoring devices.[1] According to accepted sensing mechanisms[2] grain-size reduction increases the sensitivity of the semiconducting oxides to the detection of gases. SnO_2 has, in addition, other applications, as, for instance, in transparent electrodes and optoelectronic devices.

The preparation of thick films, or sintered materials, from powders, often involves annealing in different atmospheres which results in materials with different optical and/or structural properties. The knowledge and understanding of the processing induced changes at a local scale would enable one to improve the material properties related to the mentioned applications.

In this work SnO_2 ceramic thick films were prepared from commercial powders and the influence of the sintering parameters, as annealing temperature, atmosphere and annealing time on the microstructure, defect distribution and luminescence of the samples has been investigated. Characterization with spatial resolution has been performed by means of the secondary electron and cathodoluminescence (CL) modes in the scanning electron microscope (SEM). In addition the samples were characterized by x-ray diffraction (XRD).

II. EXPERIMENT

The starting material used was commercial SnO_2 powder (Aldrich Chemical Company Inc., 99.9% purity). The powder consisted of particles and aggregates of rounded particles with sizes of about 200 nm. In order to reduce and obtain a more homogeneous particle size, the powder was milled in a centrifugal ball mill, Retsch S100, with 20-mm-diam agate balls for times of 30, 60, and 100 h, respectively. The untreated and the milled powders were compacted under a compressive load of 2 tons to form disk shaped samples of about 7 mm diameter and 2 mm thickness. Some of the samples were then sintered in air at temperatures between 1000 and 1500 °C. Some of the air sintered samples were subsequently annealed in oxygen at 600 and 900 °C.

The samples were observed in the secondary electron and CL modes in a Hitachi S-2500 or a Leica 440 SEM at accelerating voltages ranging from 10 to 30 kV, at a temperature of 80 K. For the CL measurements a Hamamatsu R-928 photomultiplier was used. The CL spectra were recorded either with the photomultiplier tube attached to an Oriel 78215 computer controlled monochromator or with a charge coupled device camera with a built-in spectrograph (Hamamatsu PMA-11). Additional structural information on the samples was obtained by x-ray diffraction.

III. RESULTS

Ball milling causes a reduction of the original particle size as observed in the SEM. The size after 30 h milling was about 130 nm and slightly smaller after 60 and 100 h milling. The sintered samples have irregular shaped grains with different sizes and porosity as a function of the annealing temperature and milling time of the starting powder. The annealing time has been found to have only a slight influence on the final grain size in the range of times, between 2 and 10 h, used in this work. Also the morphology and grain size were found to be independent of the annealing atmosphere for treatments in air, argon, and oxygen.

To study the effect of the annealing temperature a set of samples was sintered in air from the starting powder without mechanical treatment at temperatures between 1000 and 1500 °C for 10 h. The SEM images of Fig. 1 show the evolution of the morphology of these samples with the annealing temperature. The final crystal size ranges from about 200 nm

[a]Author to whom correspondence should be addressed; electronic mail: cremades@fis.ucm.es

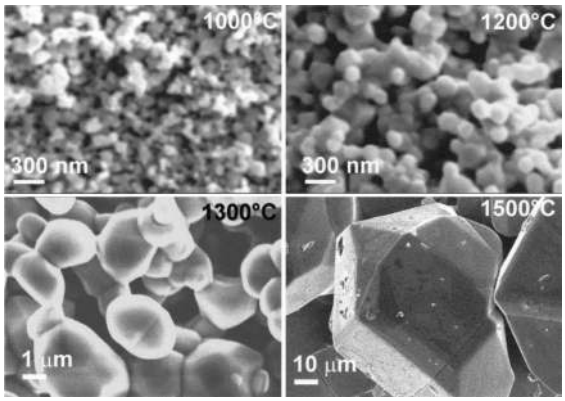

FIG. 1. Secondary electron images of samples sintered at different temperatures.

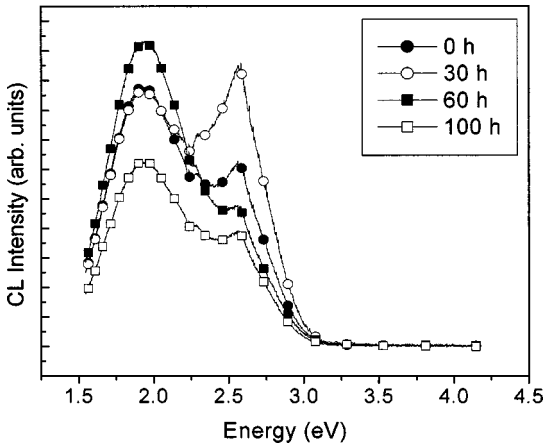

FIG. 3. CL spectra of samples with different milling times.

after the 1000 °C treatment to about 100 μm, in samples treated at 1500 °C. In the larger crystals of the samples treated at 1500 °C a well defined crystallographic form is observed. In these samples with larger crystal size, charge effects appear during observations in the SEM revealing a reduced electrical conductivity. The XRD patterns of this series of samples show the increase of the (112) and (321) textures after the 1500 °C annealing but no phase transformation is detected.

The total CL intensity of the samples depends on the annealing temperature. After the 1200 °C treatment an intensity increase is observed while the 1500 °C annealing causes an intensity reduction.

Figure 2 shows representative CL spectra of the series of samples sintered in air as compared with the spectrum of the starting powder. Gaussian deconvolution of the spectra shows the presence in the different spectra of bands centered at about 1.94, 2.25, and 2.58 eV. Spectra of the starting powder and of samples sintered at 1000 and 1100 °C are qualitatively similar with the main band peaked at 1.94 eV. For simplicity the spectra of the two latter samples are not represented in Fig. 2. The sample treated at 1200 °C shows the increase of the 1.94 eV band accompanied by a redshift of the peak to 1.90 eV. At higher temperatures the intensity of this band decreases and either the 2.58 or the 2.25 eV bands become dominant, as shown in Fig. 2. The samples sintered in air were further annealed in oxygen for 2 h at 600 and 900 °C, respectively. These treatments produced either relative increase or decrease of the 1.94 eV band depending on the sintering temperature of the sample, but no charge effects, related to a reduced conductivity, were observed in the SEM.

The effect of the previous milling time of the powders on the luminescence of the sintered samples is shown in Fig. 3. It is observed that the shorter milling time of 30 h causes the relative increase of the 2.58 eV emission which decreases again by increasing milling time.

The large grain size and the well defined crystallographic faces in the samples sintered at 1500 °C enabled us to record CL spectra on different faces of the crystals and to record CL images in which the luminescence distribution at the grain boundaries is revealed. Figure 4 shows a crystal of one of these samples and the corresponding CL spectra recorded in two faces. The spectrum recorded in the face labeled B is the representative spectrum of the samples sin-

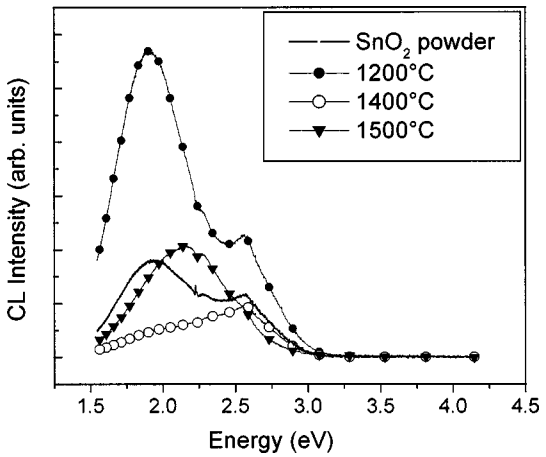

FIG. 2. CL spectra of initial powder and samples sintered at different temperatures.

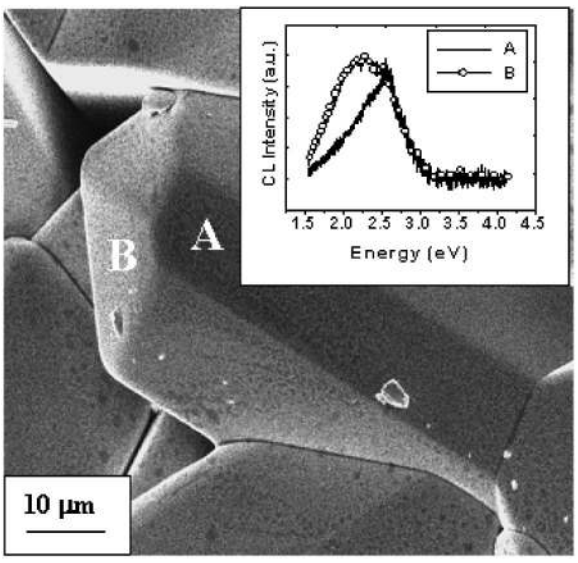

FIG. 4. CL spectra recorded at different faces of a single crystal.

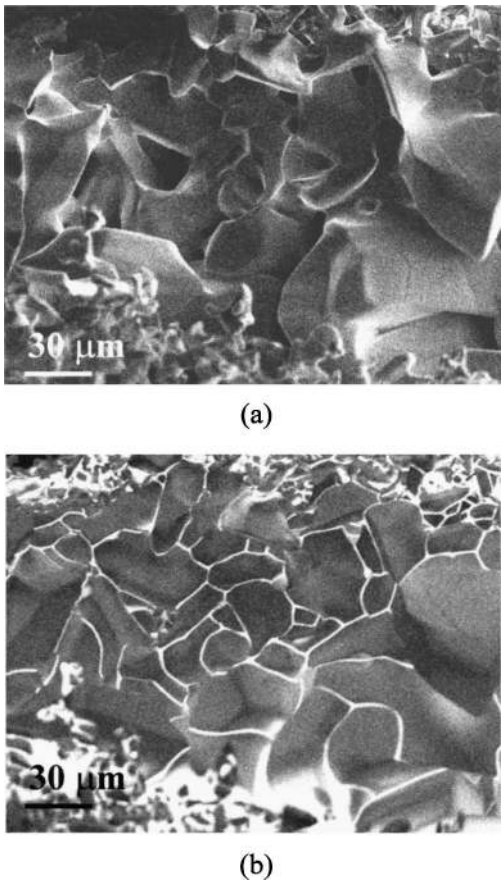

FIG. 5. SEM and CL images showing bright grain boundaries in 1500 °C sintered samples.

tered at 1500 °C with a band peaked at about 2.25 eV, which is also shown in Fig. 2. The spectrum of the face A shows a maximum at about 2.58 eV. CL images at lower magnification of the same sample show an enhanced emission at the grain boundaries (Fig. 5).

IV. DISCUSSION

The grain size increases with the sintering temperature in the series of samples sintered in air but only after the treatment at 1500 °C, texture changes and formation of crystals with well developed faceted structure are observed. The formation of large crystals at high sintering temperature is in agreement with previous observations.[3] The differences in the luminescence behavior of this series of samples would be related to the defect structure of the samples and its possible relationship with grain size and grain orientation.

The CL spectra of the starting powder and of samples sintered at temperatures up to 1300 °C show two main luminescence bands peaked at about 1.94 and 2.58 eV, respectively. An orange emission band, with maximum in the range 1.95–2 eV, has been reported in previous photoluminescence (PL) and CL studies of tin oxide. Fillard and de Murcia[4] suggested a possible coordinate-configuration model for the observed green (2.48–2.25 eV) and orange (2.0 eV) PL bands, with the transitions corresponding to a common excited state down to two possible fundamental configurations. Chang and Park[5] reported an orange PL band which was suggested to be related to nonstoichiometry and other defect states. In Ref. 6 it has been found that defect states of the most stable $SnO_2(110)$ surface correspond to donor defect states at 1.4 eV above the top of the valence band, which is compatible with transitions leading to orange emission. Crabtree[7,8] reported a broad featureless CL band in SnO_2 extending in green and orange spectral regions and suggested that is due to oxygen vacancies.

As described above, the orange band, peaked in our case at 1.94 eV, has a complex behavior during treatments in air and oxygen which would be related to changes in stoichiometry and defect structure. The band was found to increase during sintering in air at temperatures up to about 1200 °C. The later oxygen treated samples did not show noticeable resistivity increase, as observed by the absence of charge effects in the SEM, which suggests that not significant reduction in oxygen vacancy concentration takes place during the treatments, although strong intensity changes of the 1.94 eV band are observed. Since oxygen vacancies act as shallow donors in SnO_2 with an energy of about 30 meV below the conduction band,[9,10] a reduction in oxygen vacancy concentration would cause a resistivity increase. On the other hand, the fact that sintering in air at 1500 °C causes the quenching of the orange band and an associated resistivity increase, indicates that a component of the orange band is related to the presence of oxygen vacancies.

As Fig. 2 shows, treatments causing the quenching of the orange band lead to a dominant green emission in the spectra, which indicates a different origin for the green (2.25 eV) and orange (1.94 eV) emissions observed here. Comparison of the CL spectra with the sample morphology shows that the quenching of the orange band and the appearance of the green emission are associated with the formation of large crystals with well defined crystallographic faces. The influence of the crystal orientation on the CL spectra is evidenced in Fig. 5, which shows spectra recorded in two different faces. One of the spectra shows the green band which corresponds to the dominant average emission from the sample. The influence of the crystal face is due to the different adsorption processes and the different nature of the defect levels as a function of the atomic structure of the face. A strong dependence of the CL spectra on the crystal face studied has been also observed in ZnO.[11] The CL image of Fig. 5 shows that the green emission is preferentially associated with the grain boundaries. Since, as mentioned above, the oxygen vacancies appear to be associated with orange luminescence, they would not be the point defects involved in the decoration of the grain boundaries. These observations agree with the models of oxide varistors, including SnO_2 based varistors, which consider the grain boundaries as oxygen rich regions.[12]

In addition to the green and orange bands, the CL spectra show a band peaked at about 2.58 eV which has been observed to increase or even to become dominant after some of the sintering treatments in air or during ball milling for 30 h, as Fig. 3 shows. As the green band, this emission is associated with certain crystal faces in the samples sintered at 1500 °C (Fig. 4). A luminescence band at 2.58 eV could be present as a component in the broadband reported by some

authors, e.g., in Ref. 4, but is not normally reported as a resolved band independent of the green and orange bands. In Ref. 5 a PL emission band is observed at 2.58 eV but it appears at 20 K as a consequence of an energy shift of the orange band at low temperature. On the contrary, the 2.58 eV band observed in this work is not related to the orange luminescence band and is present at 80 K and higher temperatures. It appears then to be related to defects, different than oxygen vacancies, which form mainly in specific crystal faces.

Figure 3 shows that mechanical milling has a marked influence on the 1.94 and the 2.58 eV bands which have different behavior during milling. This confirms the different mechanisms related to both emissions. Milling for 30 h causes the enhancement of the 2.58 eV band that becomes the main band of the spectrum. Increasing the milling time to 60 and 100 h leads to a relative reduction of the 2.58 eV band as well as the reduction of the total CL intensity. The same qualitative behavior, intensity increase for the first steps of milling and decrease during long time milling, is observed for the 1.94 eV. The increase of this band is observed, however, only after 60 h treatment and the decrease is revealed in the 100 h milled sample. These results show that both bands are related to defects generated during plastic deformation. The recovery effect observed for long milling times, which has been previously found in luminescence studies of milled ZnO,[13] would be a consequence of the competition between defect creation and recovery which takes place during milling.[14] Mechanical milling induces the reduction of particle size as well as of the grain size of the grains forming the particles observed in SEM. This could lead to the appearance of luminescence related to quantum size effects as has been observed in ball milled Si[15] and Ge.[16] In the present work the luminescence spectra of the milled samples did not reveal the existence of quantum size effects. A similar result was found in Ref. 13 for ball milled nanocrystalline ZnO. Quantum size effects have been proposed to interpret the violet band at 2.88 eV appearing in SnO_2 obtained by spark processing.[5]

V. CONCLUSIONS

CL of sintered SnO_2 shows the presence of bands at 2.58, 2.25, and 1.94 eV whose relative intensities depend on the sintering treatment. Local CL spectra show that the 2.25 and 2.58 eV emissions are preferentially related to specific crystal faces. CL images reveal that the green (2.25 eV) band is mainly associated with grain boundaries. The results indicate that the orange (1.94 eV) band, which has a different origin than the green band, is complex and one of its components appears to be related to oxygen vacancies. Mechanical milling induces strong changes in the intensity of the CL bands at 1.94 and 2.58 eV. The evolution of these bands with milling time shows the existence of formation and recovery of defects during milling.

ACKNOWLEDGMENTS

This work has been supported by MCYT (Project No. MAT 2000-2119). D. M. acknowledges a grant from MCYT.

[1] G. Martinelli, M. C. Carotta, E. Traversa, and G. Ghiotti, MRS Bull. **24**, 30 (1999).
[2] C. Xu, J. Tamaki, N. Miura, and N. Yamazoe, Sens. Actuators B **3**, 147 (1991).
[3] H. J. Van Daal, Solid State Commun. **6**, 5 (1968).
[4] J. P. Fillard and M. de Murcia, Phys. Status Solidi A **30**, 279 (1975).
[5] S. S. Chang and D. K. Park, Mater. Sci. Eng., B **95**, 55 (2002).
[6] J. M. Themlin, R. Sporken, J. Darville, R. Caudano, and J. M. Gilles, Phys. Rev. B **42**, 11914 (1990).
[7] D. F. Crabtree, J. Phys. D **7**, L22 (1974).
[8] D. F. Crabtree, J. Phys. D **7**, L17 (1974).
[9] E. De Frésart, J. Darville, and J. M. Gilles, Surf. Sci. **126**, 518 (1983).
[10] D. F. Cox, T. B. Fryberger, and S. Semancik, Phys. Rev. B **38**, 2072 (1988).
[11] A. Urbieta, P. Fernández, Ch. Hardalov, J. Piqueras, and T. Sekiguchi, Mater. Sci. Eng., B **91–92**, 345 (2002).
[12] P. R. Bueno, E. R. Leite, M. M. Oliveira, M. O. Orlandi, and E. Longo, Appl. Phys. Lett. **79**, 48 (2001).
[13] R. Radoi, P. Fernández, J. Piqueras, M. Wiggins, and J. Solís, Nanotechnology **14**, 794 (2003).
[14] C. C. Koch, Nanostruct. Mater. **2**, 109 (1993).
[15] C. Díaz-Guerra, A. Montone, J. Piqueras, and F. Cardellini, Semicond. Sci. Technol. **17**, 77 (2002).
[16] E. Nogales, A. Montone, F. Cardellini, B. Méndez, and J. Piqueras, Semicond. Sci. Technol. **17**, 1267 (2002).